SOSTDC1 Promotes Invasion and Liver Metastasis in Colorectal Cancer via Interaction with ALCAM/CD166

Rubén A. Bartolomé[1†], Laura Pintado-Berninches[1], Marta Jaén[1], Vivian de los Ríos[1], Juan Ignacio Imbaud[2], and J. Ignacio Casal[1*]

1. Department of Molecular Biomedicine, Centro de Investigaciones Biológicas, CSIC, Ramiro de Maeztu 9, 28039 Madrid, Spain
2. Protein Alternatives S.L., Tres Cantos, Madrid, Spain

†.- Co-corresponding author

Running title: SOSTDC1 associates with ALCAM to promote liver metastasis

Keywords: SOSTDC1, ALCAM, BMP4, colorectal cancer, liver metastasis

Words: 4710

*. Corresponding author:
J. Ignacio Casal
Department of Cellular and Molecular Medicine
Centro de Investigaciones Biológicas (CIB-CSIC)
Ramiro de Maeztu, 9
28040 Madrid, Spain
Phone: +34 918373112
Fax: +34 91 5360432
Email: icasal@cib.csic.es

ABSTRACT

The mechanistic basis of liver metastasis in colorectal cancer remains poorly understood. We previously reported that the sclerostin domain containing-1 (SOSTDC1) protein is overexpressed in the secretome of metastatic colorectal cancer cells and can inhibit liver homing. Here, we investigated the mechanisms of SOSTDC1 for promoting invasiveness and progression of colorectal cancer liver metastasis. SOSTDC1 inhibition of BMP4 maintains the expression of cancer stem cell traits, including SOX2 and NANOG. Immunoprecipitation and mass spectrometry analyses reveal the association of SOSTDC1 with ALCAM/CD166, which was confirmed by confocal microscopy and competition ELISA. Interaction with ALCAM is mediated by the N-terminal region of SOSTDC1, which contains a sequence similar to the ALCAM-binding motif used by CD6. Knocking down either SOSTDC1 or ALCAM expression, or using blocking antibodies, reduces the invasive activity by inhibiting Src and PI3K/AKT signaling pathways. In addition, ALCAM interacts with the α2ß1 and α1ß1 integrins, providing a possible link to Src activation. Finally, inoculation of SOSTDC1-silenced metastatic cells increases mouse survival by inhibiting liver metastasis. In conclusion, SOSTDC1 promotes invasion and liver metastasis in colorectal cancer, by overcoming BMP4-specific anti-metastatic signals and inducing ALCAM-mediated Src and PI3K/AKT activation. These experiments underscore the potential of SOSTDC1 as a therapeutic target in metastatic colorectal cancer.

INTRODUCTION

Metastasis is a complex process that involves several steps, from extravasation to colonization at new organs, and requires the coordinated action of a large number of proteins to modulate different effects on adhesion, migration, invasiveness, and survival in the target organ [1]. Increasing evidence suggests that cancer metastasis is promoted by a small number of cancer stem cells (CSCs) that undergo self-renewal and differentiation to promote tumor growth [2]. Only CSCs can reinitiate tumor growth after reaching the target organs [3]. Recently, we have used the KM12 colorectal cancer cell model to analyze which proteins are relevant in metastasis [4]. KM12SM and KM12L4 are highly metastatic colorectal cancer cells that exhibit features of CSCs as they overexpress CSC markers, (e.g. CD44, CD133, and EPCAM), as compared to non-metastatic KM12C cells [5, 6]. Using proteomic analysis, we found increased expression levels of SOSTDC1 (sclerostin domain–containing-1, a.k.a. USAG1 or ectodin), EFNA3, and CD137L in the secretome of KM12SM cells, providing three promising candidates for dissecting the mechanisms of metastatic colonization [7]. However, SOSTDC1 was the only secreted protein and the less characterized in metastatic dissemination among the three candidates. In addition, SOSTDC1 stimulated the migration, invasive ability and liver homing capacity of colorectal cancer metastatic cells, but did not promote proliferation or primary tumor growth [7].

SOSTDC1 belongs to the DAN (differential screening-selected gene aberrant in neuroblastoma) protein family, which also includes SOST, Gremlin-1, Coco, and Cerberus-1 (among others). These proteins inhibit the bone morphogenetic proteins (BMPs) of the TGFβ family [8, 9]. SOSTDC1 is a secreted protein with a glycosylated N-terminus that

contains a C-terminal cysteine knot (CTCK) domain [10]. Of note, this domain is present in numerous growth factors, including TGFβ, NGF, PDGF, vWF, NDP, and mucin-2, and is involved in dimerization, receptor binding, and signal transduction. SOSTDC1 negatively regulates BMP signaling during cellular proliferation, differentiation, and apoptosis in several biological processes (such as dentary morphogenesis, embryo implantation in the endometrium, and healing of bone fractures) [8]. In addition, SOSTDC1, and its orthologue Wise, modulate various processes, in development as well as in cancer, through the regulation of the Wnt pathway [8, 11].

SOSTDC1 expression has been shown to be reduced in primary tumors of renal [12], breast [13], prostate cancer [14], and non-small cell lung cancer [15] as compared to normal tissue. However, none of these studies explored differences of SOSTDC1 expression between metastatic and primary tumors, and only a few reports described SOSTDC1 expression in metastatic cells[16, 17]. A critical step in organ colonization during metastasis is to subvert the cellular programs that impose a state of dormancy on the metastatic cells in the receptor organ, which is usually imposed by BMPs or other members of the TGFβ pathway. The BMP antagonists Coco and Gremlin1 act as a counterbalance for BMP signaling in breast cancer and glioblastoma, respectively, enabling maintenance of CSCs and reactivating metastatic colonization or invasive growth [18, 19]. However, the effects of SOSTDC1 in regulation of liver metastasis are totally unknown, and further clarifications, beyond its capacity of inhibiting BMP4, are necessary. We should also take into account that late-stage colorectal cancer-derived cell lines display mutational inactivation of the TGF-β pathway, and that KM12SM and L4 cells carry biallelic *TGFBR2* loss-of-function mutations and do not respond to TGF-β [20], which may affect BMP signaling.

Here, we have characterized the mechanisms of action of SOSTDC1 in colorectal cancer cells and how they impact metastasis. Notably, we observed the capacity of SOSTDC1 to work as a novel ligand of ALCAM to promote invasion and facilitate liver metastasis in colorectal cancer through activation of the Src-PI3K/AKT pathways. Our results highlight the potential of SOSTDC1 as a candidate therapeutic target.

RESULTS

SOSTDC1 is overexpressed in late stages of colorectal cancer

We first examined the expression of SOSTDC1 in eight colon cancer cell lines. Metastatic cell lines expressed SOSTDC1in cell lysates, and to a greater extent in the conditioned media, in its secreted form (**Fig. 1A**). To study its clinical value, we checked SOSTDC1 expression in tumor and adjacent healthy tissue in colon cancer patients as well as in paired normal and metastatic liver samples. Normal colon tissue exhibited higher levels of SOSTDC1 expression than primary tumors. However, the highest expression was found in metastatic tissues (**Fig. 1B**). By immunohistochemistry, SOSTDC1 expression in liver metastasis was significantly higher than in primary tumors (**Fig. 1C**). This indicates that SOSTDC1 expression declined in early stages of colorectal cancer, but increased in liver metastasis, underscoring the potential clinical value of determining its expression levels.

SOSTDC1 promotes cell invasion through the Src, PI3K/AKT, and JNK pathways

Next, we explored the contribution of SOSTDC1 to the invasive properties of SW620, KM12SM, or KM12L4 cells that had been transiently-silenced for SOSTDC1 with two different siRNAs (for SW620 and KM12SM), or stably silenced with two lentiviruses (for KM12L4) (**Fig. 2A**). A clear reduction in the cell invasion capacity through Matrigel was observed for SOSTDC1-silenced cells (**Fig. 2B**). A similar inhibition was obtained with a polyclonal anti-SOSTDC1 (**Fig. 2C**). To define the molecular underpinnings of SOSTDC1, we investigated its capacity to activate the Src and PI3K/AKT pathways in the cell lysates of metastatic cells. All three cell lines showed a significant decrease in the activation of Src and AKT after SOSTDC1 silencing. Stably-silenced cells exhibited a major decline in the

activation of all the signaling proteins, including phospho-JNK. However, ERK phosphorylation was not reduced in SW620 cells, and an effect on JNK activation was observed only in KM12L4 cells (**Fig. 2D**). To confirm the signaling pathways involved in SOSTDC1-mediated invasion we tested different inhibitors in SW620, KM12SM and SOSTDC1-silenced or scrambled KM12L4 (**Fig. 2E**). The increased invasion induced by SOSTDC1 was strongly reduced by inhibitors of Src (PP2) or PI3K (LY294002). In agreement with the observed JNK activation, invasion was partially reduced by JNK inhibitor II in KM12L4 cells, but not in KM12SM or SW620 cells. In the three cell lines, invasion was not affected by UO126 (a MEK1/2 inhibitor). Together, these findings confirm that SOSTDC1-regulated invasion was mediated by the Src and PI3K/AKT pathways.

SOSTDC1 inhibits BMP4 to maintain expression of stem cell transcription factors

Next, we explored the effects of BMP4 on the SOSTDC1-mediated invasive capacity. SOSTDC1-silenced or scrambled KM12L4 cells treated with SOSTDC1 (10 ng/mL) showed a clear increase in their invasive capacity, which was inhibited by BMP4 addition, in a dose-dependent manner (**Fig. 3A**). To define the capacity of SOSTDC1 to regulate BMP signaling in colorectal cancer metastatic cells, we characterized the expression of BMP receptors and the activation status of the downstream target SMAD5. Both receptor subunits (BMPR-IB and BMPR-II) were expressed in KM12SM cells, only BMPR-II in KM12L4 cells, and neither in SW620 cells (**Fig. 3B**); thus, as a functional BMP receptor requires a heterodimer of receptor types I and II, only KM12SM were expected to respond to BMPs. To assess BMP signaling, cells were silenced for SOSTDC1 and exposed to increasing concentrations of BMP4. BMP4 increased pSMAD5 only in KM12SM cells (but

not in KM12L4 or SW620), and only when high amounts of BMP4 (50-250 ng/mL) were used in SOSTDC1-silenced cells (**Fig. 3B**). Thus, endogenous SOSTDC1 expression was sufficient to block the effects of BMP4. Of note, stably SOSTDC1-silenced KM12L4 cells had less pSMAD5 than control transfectants.

We next examined the capacity of SOSTDC1 to promote tumor sphere formation and to sustain expression of stem cell transcription factors. Neither treatment with SOSTDC1, or its inhibition with BMP4 altered the colony formation capacity (**Fig. 3C**). In contrast, SOSTDC1-silenced KM12L4 cells or KM12SM cells treated with BMP4, showed significantly inhibited the expression of the pluripotent-associated transcription factors, such as SOX2, NANOG, EPCAM, BMI1, and ABCF1 (**Fig. 3D**). OCT4 was undetectable. Collectively, these results indicated that i) SOSTDC1 and BMP4 have antagonistic actions in metastasis and ii) the capacity of SOSTDC1 to maintain the pluripotent status of colorectal CSCs avoiding the inhibitory effect of BMP4.

SOSTDC1 interacts with ALCAM via a CD6-like motif

Beyond its interaction with BMP4, SOSTDC1 is likely to interact with other proteins to regulate invasion. Therefore, we investigated the SOSTDC1 protein interaction network by immunoprecipitation followed by mass spectrometry. Cell lysates from metastatic SW620 cells were immunoprecipitated with anti-SOSTDC1, or an irrelevant antibody as a negative control. After removing ribosomal and proteasomal proteins, we identified 21 proteins likely to specifically interact with SOSTDC1 (**Supplementary Table S1**). Among the interacting proteins, we identified ALCAM, CEACAM5, talin-2, and PI3K-related proteins, as well as secreted proteins, such as the serpins B6 and B12 (**Fig. 4A)**. With

167 respect to its molecular function, some of the interacting proteins were involved in cell
168 adhesion, migration, and invasion (NHERF1, ARPC4, and PAFAH1B1) and in the PI3K
169 and Rho-GTPase signaling pathways. The association with CEACAM5, ALCAM, AKT,
170 BMP4, mTOR, NHERF1, and RAC1 was verified by immunoprecipitation and Western
171 blot in SW620 and KM12SM cells (**Fig. 4B**).

172 Functionally, SOSTDC1-interacting proteins included cell-cell adhesion molecules
173 (i.e. CEACAM5, ALCAM), secreted proteins and proteins related with the cytoskeleton,
174 actin polymerization, or microtubules activities. Apart from intracellular proteins, we
175 excluded CEACAM5 from further analysis due to very limited information about
176 CEACAM5 interactions. ALCAM is a cell adhesion molecule associated with stemness,
177 cancer progression, and poor prognosis in colorectal cancer [21, 22]. Therefore, ALCAM might
178 be the link between SOSTDC1 and the cytoskeleton interacting proteins. ALCAM and its
179 canonical ligand CD6 [22] play a role in the immunological synapsis. Notably, we identified
180 motifs similar to CD6 binding sequences in the N-terminal sequence of SOSTDC1 (**Fig.**
181 **4C**). We therefore built an *in silico* model of SOSTDC1 based not only on its paralog
182 SOST but also the PEP-FOLD 3 program for its N-terminal region, due to the low
183 homology (<50%) between SOSTDC1 and SOST in such region. The *in silico* model
184 predicted that the three SOSTDC1 sequences similar to those used for CD6 binding to
185 ALCAM [22] are in close proximity after protein folding, even though two are located in the
186 N-terminal region and one in loop 1 (**Fig. 4D**). Confocal microscopy showed significant
187 co-localization of both proteins in membrane staining pattern (of 77.1%) (**Fig. 4E**).
188 Indirect ELISA revealed that soluble SOSTDC1 can bind coated ALCAM in a dose-
189 dependent manner (**Supplementary Fig. S1A**). Further, the homotypic binding

ALCAM/ALCAM was inhibited after adding increasing amounts of soluble SOSTDC1 (**Supplementary Fig. S1B**). Flow cytometry showed that ALCAM siRNA silencing caused a clear reduction in the level of SOSTDC1 attached to the cell membrane in SW620 and KM12SM metastatic cell lines (**Figs. 4F, 4G**). Collectively, these results provide strong evidence that SOSTDC1 binds ALCAM in metastatic colorectal cancer cells.

Truncation of the SOSTDC1 N-terminus inhibits ALCAM-mediated migration and invasion

To further demonstrate that the binding of SOSTDC1 to ALCAM is mediated through the "CD6-like" binding sequence, we prepared an amino-terminally truncated variant of SOSTDC1 (ΔN67-SOSTDC1), lacking the first 67 residues and two of the three ALCAM binding sequences (**Supplementary Fig S2**). In contrast to the wild-type (WT) SOSTDC1, ΔN67-SOSTDC1 did not bind the cell membrane (**Fig. 5A**). Moreover, whereas SOSTDC1 was a potent chemoattractant for colon cancer cells invasion, ΔN67-SOSTDC1 failed to promote cell invasion (**Fig. 5B**). Cell migration and invasion are initiated by the formation of protrusive structures (e.g., filopodia, lamellipodia, or invadopodia) that require polymerization of actin filaments [23]. The mutant ΔN67-SOSTDC1 did not promote a significant increase in F-actin content (**Fig. 5C**). Testing for Src and PI3K activation pathways in the metastatic cell lines treated with SOSTDC1 or ΔN67-SOSTDC1 revealed a fast increase (5 min) in Src, AKT, and ERK phosphorylation (and thus pathways) in all cell lines treated with SOSTDC1, including JNK phosphorylation in KM12L4-stably silenced cell, while no increase was observed with ΔN67-SOSTDC1 (s (**Fig. 5D**). Together, these results confirm that the N-terminal region of SOSTDC1 is necessary for its binding to ALCAM, and its ability to promote cell migration and invasion.

ALCAM regulates cell invasion and actin polymerization in a coordinated way with SOSTDC1

Knocking down either ALCAM (**Fig. 6A)** or SOSTDC1 in SW620 or KM12SM cells drastically reduced the invasive behavior of both cell lines (**Fig. 6B, Supplementary Fig. S3**). Moreover, the simultaneous silencing of both proteins did not cause a cumulative effect in cell invasion, suggesting that both proteins likely use the same mechanisms/ signaling pathways in invasion. Notably, F-actin content analysis in SW620 or KM12SM cells silenced for ALCAM or SOSTDC1 revealed that interfering with the expression of either protein caused a similar, intense reduction in F-actin levels (**Fig. 6C**). Further, treating ALCAM-silenced cells with recombinant SOSTDC1 showed no activation of the Src, AKT and ERK pathways in KM12SM cells (**Fig. 6D**), demonstrating the dependence of SOSTDC1 for the ALCAM receptor. ALCAM-ALCAM interactions can activate or not metalloproteinases to promote cell invasion [24, 25]. Here, colorectal cancer cells showed no differences in the expression and activation of MMP2 and MMP9 after SOSTDC1 silencing (**Supplementary Fig. S4**), suggesting MMP-independent SOSTDC1-mediated invasion mechanisms.

To explore the connection between ALCAM and the SRC-PI3K/AKT signaling pathways we carried out immunoprecipitation of ALCAM. Western blot results indicated the presence of the α2 and α1 (but not α3) integrins, in the ALCAM immunoprecipitates. CD9, a tetraspanin reported to interact with ALCAM, was also present in the interactome (**Fig. 6E**). Finally, we investigated the expression of ALCAM in clinical metastatic samples. We observed a significant association between increased expression levels of ALCAM and

liver metastasis (**Fig. 6F**). Together, these results suggest that SOSTDC1 and ALCAM use identical pathways for promoting invasion and metastasis.

SOSTDC1 expression correlates with ALCAM expression in metastasis, and SOSTDC1 silencing reduces liver metastasis in mouse models

We next explored the coordinated expression of SOSTDC1 and ALCAM in colorectal cancer metastasis using a public transcriptomic database with more than 500 patients. After normalization and calculation of z-scores (**Supplementary Fig. S5**), we found a significant correlation between high expression levels of SOSTDC1 or ALCAM and metastasis in patients (**Fig. 7A**). Correspondingly, patients with low expression levels showed a lower presence of metastasis (between 3–6%) than patients with high expression of SOSTDC1 or ALCAM (12%).

Finally, to investigate the potential therapeutic value of SOSTDC1 in a mouse model of metastasis, we injected either parental or SOSTDC1-knocked down (KD) KM12L4 cells into the spleen of Swiss nude mice. Only one of the mouse inoculated with KD cells died from metastasis (**Fig. 7B**). Further, all mice inoculated with parental cells developed macroscopic liver metastasis, but only one with SOSTDC1-silenced cells developed a tumor (with a small node in the liver) (**Fig. 7C**). In addition, we observed a massive reduction in the liver volume occupied by metastasis in mice inoculated with SOSTDC1-silenced cells (**Fig. 7C**). Thus, SOSTDC1 is relevant for establishing liver metastasis, making it a potential therapeutic target of high interest for colorectal cancer.

DISCUSSION

We found that SOSTDC1 is overexpressed in metastatic cell lines and liver metastasis, and acts as a novel ligand of ALCAM to promote colorectal cancer metastasis. The effects of SOSTDC1 on invasion and metastasis were mediated by ALCAM as well as the activation of the Src and PI3K/AKT pathways, likely through the additional interaction of ALCAM with α2ß1 or α1ß1 integrins (**Fig. 7D**). Therefore, SOSTDC1 seems to activate a large protein complex formed by ALCAM, CD9 and ß1 integrins (and perhaps other proteins). Indeed, knocking down SOSTDC1 in metastatic cells significantly increased mouse survival and reduced liver metastasis.

The initial decline of SOSTDC1 expression in colorectal cancer, followed by expression recovery at late stages, is likely to be epigenetically regulated in a reversible way, similar to the epithelial-to-mesenchymal transition (EMT)-MET programs that promote a mesenchymal phenotype at the initial cancer stages followed by a recovery of the epithelial phenotype at the late stages. Indeed, the transcriptional regulation of SOSTDC1 was epigenetically regulated in gastric [26, 27] and prostate cancer cells [14]. Some reports have described that reduction of SOSTDC1 in primary tumors is associated with poor outcome [16, 17, 28]. In contrast, we observed that an initial decline in SOSTDC1 expression in the primary tumors of colorectal cancer had no significant impact on prognostic value. According to the Human Protein Atlas database (https://www.proteinatlas.org/ENSG00000171243-SOSTDC1/pathology), SOSTDC1 expression can be associated with a better or worse outcome, depending on the cancer type, indicating that SOSTDC1´s role in metastasis and its value for prognosis are cancer type-specific. Moreover, in those carcinomas lacking ALCAM (e.g. NSCLC, gastric) both the

278 role of SOSTDC1, as well as the molecular mechanisms of migration, invasion and
279 proliferation are likely to be distinct from those in colorectal cancer. Indeed, metastatic
280 colonization by different tumors seems to require organ-specific BMP antagonists: Coco
281 for lung metastasis in breast cancer [18], Noggin for bone metastasis in prostate cancer [29] and
282 SOSTDC1 for liver metastasis in colorectal cancer.

283 Although SOSTDC1 is usually classified as a BMP inhibitor, our evidences now
284 indicate that SOSTDC1 and BMP4 have antagonistic effects on cancer metastasis. Indeed,
285 addition of BMP4 inhibited SOSTDC1-promoted colorectal cancer invasion, and
286 SOSTDC1 inhibited anti-metastatic signals of BMP4. Of note, BMP4 signaling through
287 SMAD proteins seemed severely impaired in the metastatic cells, except KM12SM, in
288 which BMP4 promotes SMAD5 phosphorylation only in absence of SOSTDC1. Therefore,
289 both proteins antagonize each other, inhibiting the binding to their respective receptors.
290 Likely, in metastatic colorectal cancer, the balance would favor the pro-metastatic effect of
291 SOSTDC1 over the inhibitory activity of BMP4. We observed a few similarities between
292 SOSTDC1 in metastatic colorectal cancer cells with the effects of Coco in lung metastasis
293 in breast cancer cells[18]: i) SOSTDC1 promotes metastatic colonization without increasing
294 the proliferation of the primary tumor cells [7], and ii) SOSTDC1 sustains the expression of
295 stem cell transcription factors, like SOX2 and NANOG [30]. In aggressive and metastatic
296 cancer cells, a reactivation of these transcription factors is required for maintaining the
297 pluripotent embryonic stem cell phenotype [31]. Therefore, SOSTDC1 supports the
298 reactivation of colon cancer stem cell traits, and thus consequently the capacity for self-
299 renewal and propagation, of the CSCs by inhibiting BMP suppressing effects on NANOG
300 and SOX2.

Beyond the inhibition of BMP4, we have demonstrated that SOSTDC1 and ALCAM associate with each other, and that this association is relevant for invasion and metastatic progression. These conclusions were based on the following results: i) ALCAM was immunoprecipitated with SOSTDC1, ii) SOSTDC1 and ALCAM co-localized on the surface of cancer cells and compete with each other for binding, iii) binding to ALCAM was mediated through the N-terminal region of SOSTDC1, and iv) silencing of either SOSTDC1 or ALCAM caused a similar decline in Src and AKT signaling activation, actin polymerization, and cell invasion. The effects of ALCAM on the Src and AKT signaling might be explained by the ALCAM association with a cluster of ß1 integrins (including α2 and α1), facilitated by CD9; this would require the triggering of the integrin signaling pathway and, consequently, Src and PI3K/AKT activation (Fig. 7D). Notably, the Δ67N SOSTDC1 mutant inhibited invasion, actin polymerization, and cell signaling mediated by SOSTDC1 through ALCAM, confirming binding sequences for ALCAM in the N-terminus of SOSTDC1. Our findings were replicated in three cell lines with different genetic background. Together these data establish that SOSTDC1 is a ligand for ALCAM, and that both proteins cooperate in promoting invasion and liver metastasis in colon cancer.

ALCAM, EPCAM and CD44 constitute a robust panel profile for stem cell isolation from colorectal CSCs [32]. In colorectal cancer and other tumors (i.e. melanoma, pancreatic, mesothelioma), ALCAM expression correlates with a worse prognosis for patients [33-37]. ALCAM associates to the actin cytoskeleton through the ezrin/radixin/moesin (ERM) family proteins and syntenin-1, which enhances cell motility by binding to the cytosolic tail of ALCAM [38]. In this regard, our observation that ALCAM associates with CD9 should facilitate our understanding of the connection with the actin cytoskeleton [39]. Interestingly,

other proteins present in the SOSTDC1 interactome (such as NHERF1, ARPC4, and PAFAH1B1) have also been related to actin polymerization, migration, and invasion in different types of cancer. Although barely characterized, all share the capacity to promote actin polymerization and migration. The scaffold protein NHERF1 connects plasma membrane proteins with members of the ERM family, thereby linking them to the actin cytoskeleton and regulating their surface expression. ARPC4 (actin-related protein 2/3 complex subunit 4) functions as actin-binding component of the ARP2/3 complex, which is involved in regulation of actin polymerization. Silencing of ARPC4 significantly reduces cell migration in pancreatic cancer cell line [40]. PAFAH1B1 (platelet-activating factor acetylhydrolase 1B) is required for proper activation of Rho GTPases and actin polymerization [41]. PAFAH1B1 overexpression contributes to promote migration and invasiveness of lung cancer cells [42]. Another interactor, DRG1, was a component of the Coco expression signature that predicted overall relapse to the lung [18] and might be another interesting target to explore in future experiments. Other proteins of the interactome, including ATXN10, SERPINB12 and SERPINB6 remain to be better characterized for cancer metastasis.

ALCAM-ALCAM interactions act as a cell density sensor, diapedesis controller, and as an initiator of a signal that activates metalloproteinases (like MMP-2), all of which affect the cell invasion capacity [43]. Our results indicate that, in colorectal cancer cells, SOSTDC1 disrupts the ALCAM-ALCAM interaction and promotes the ALCAM-SOSTDC1 interaction relying also on CD9, which strengthens the ALCAM-CD6 interaction in leukocytes [39]. Formation of ALCAM-SOSTDC1 interactions might promote invasion in colorectal cancer through different mechanisms. Indeed, the effect of ALCAM-

ALCAM interactions in invasion remains controversial. In melanoma, constructs either lacking the N-terminal domain (ΔN-ALCAM) or a soluble domain 1 of ALCAM (sALCAM) had positive or negative effects on migration and invasion, respectively, without activation of MMP2 [24, 25]. Our results with SOSTDC1 might shed light on this apparent contradiction. First, the expression of ΔN-ALCAM would facilitate the interaction of SOSTDC1 with endogenous ALCAM, promoting migration and invasion. Second, sALCAM might bind and sequester SOSTDC1, thereby inhibiting both binding of SOSTDC1 to ALCAM and, consequently, invasion and metastatic capacity [25]. In colorectal cancer cells, SOSTDC1 does not affect the expression of the collagenases, but promotes cell invasion by disrupting ALCAM homophilic interactions, promoting actin polymerization and activating the integrin-SRC-PI3K/AKT-ERK signaling pathway. In agreement with this, ALCAM depletion leads to a reduced primary tumor size and reduced metastatic local spread in endometrioid endometrial cancer [44]. ALCAM targeting either using antibodies that interfere with ALCAM oligomerization or by delivering cytotoxic payloads have been proposed as therapies for ALCAM positive tumor types [45]. Our results suggest that blocking SOSTDC1 binding to ALCAM (via antibodies, aptamers, or peptides) might constitute a suitable and valuable strategy for metastasis inhibition.

The identification of SOSTDC1 from a proteomic analysis of the secretome of metastatic cells demonstrates the value of this type of analysis for identifying relevant proteins in metastasis. Here, we have elucidated some of the different mechanisms used by SOSTDC1 to promote invasion and liver metastasis in colorectal cancer. One mechanism depends on the capacity of SOSTDC1 for sustaining the expression of CSCs transcription factors, thus maintaining self-replication and stemness status. Another mechanism requires

370 the ability of SOSTDC1 to promote cancer invasion through its interaction with ALCAM.
371 Our results with shRNA silencing and a commercial anti-SOSTDC1 antibody showed a
372 clear inhibition of the invasive capacity in metastatic colorectal cancer cells. Although
373 further studies are necessary to validate its therapeutic value, SOSTDC1 is likely to be an
374 interesting target for therapeutic intervention in colorectal cancer metastasis.

MATERIALS AND METHODS

Cell lines, siRNAs, lentiviruses, and tumor samples

The human colon cancer cell lines KM12C (poorly metastatic) and KM12SM and KM12L4 (highly metastatic) kindly provided by Dr. I. Fidler (MD Anderson Cancer Center, Houston, TX) were authenticated by short tandem repeat analysis. SW480, SW620, LIM1215, HT-29, Colo205, and Colo320 human colon cancer cells were purchased from ATCC and passaged less than 6 months after purchase. Mycoplasma contamination was regularly excluded. Cell lines were cultured in DMEM (Invitrogen) containing 10% FCS (Invitrogen) with antibiotics at 37ºC in a 5% CO_2 humidified atmosphere. For transient transfections, control siRNAs, or two different siRNAs specifically targeting SOSTDC1 (SASI-Hs01_00149385 and SASI-Hs01_00149386) or ALCAM (SASI-Hs01_0021533 and SASI-Hs01_0021534) (Sigma-Aldrich) were transfected with JetPrime (Polyplus Transfection). Stable silencing used the GIPZ Lentiviral shRNA Transfection Starter Kit with DharmaFECT kb (Dharmacon). In brief, KM12L4 cells were infected with lentiviral particles containing two different shRNAs against SOSTDC1 (#1 RHS4430-200271487-V3LHS_386617, #2 RHS4430-200202272-V2LHS_96631) or an irrelevant shRNA (control). After 48 h, stable transfectants were selected with 5 μg/mL puromycin (Sigma-Aldrich) for 2 weeks and then maintained in 0.5 μg/mL puromycin. PP2, LY294002, UO126 and JNK inhibitor II were purchased from Sigma-Aldrich.

Nine sets of human colon cancer paired samples from primary tumor and liver metastasis and their healthy tissue counterparts were kindly provided by Dr. A. Villanueva (Institut Català d'Oncologia. Hospital Duran i Reynals). Sample collection was approved by the

Ethical Review Board of the hospital. For immunohistochemistry, a tissue microarray based on tissue samples was obtained from the Surgical Pathology Departments of Hospital Fundación Jiménez Díaz and Hospital Clínico (Madrid) after approval of the Research Ethics Committee of the hospitals. Written informed consent was provided by all patients.

Production of SOSTDC1 recombinant proteins

SOSTDC1 wild-type (wt) (aa 24–206; full sequence without the signal peptide) and variant ΔN67-SOSTDC1 (aa 68–206) were obtained by gene synthesis and cloned into pET28a (Genescript) with a 6×His tag in the C-terminal regions. Both proteins were expressed in the BL21 *E. coli* strain for 4 h at 37ºC after induction with 0.8 mM IPTG. Cell pellets were extracted by sonication in PBS buffer with 1×Complete Protease Inhibitor (Roche), PMSF, and 1 mM DTT. The soluble lysate was discarded, and the insoluble fraction of the extraction was solubilized with 6 M guanidinium chloride overnight. The solubilized proteins were clarified by centrifugation and filtration with 0.45 μm filter. SOSTDC1 and ΔN67-SOSTDC1 were purified using HisTrap FF Crude 1 mL column, following the standard on-column refolding protocol provided by the manufacturer (GE Healthcare) in an AKTA Prime Plus FPLC system. Recombinant SOSTDC1 was used at 10 ng/mL for 5 min in flow cytometry and actin polymerization assays.

Immunoprecipitation and mass spectrometry

See Supplementary Information

Cell invasion

To evaluate the invasive properties of the cancer cells, 6×10^4 cells were loaded onto 8-mm pore-size filters coated with 35 μL of Matrigel (BD Biosciences) diluted 1:3 in DMEM in Transwell plates (Sigma-Aldrich). The lower compartment of the invasion chamber was filled with DMEM–5% serum or with recombinant SOSTDC1 (10 ng/mL) in serum-free DMEM. After 48 h, non-invading cells were removed, and cells that had migrated through the filter were fixed with 4% paraformaldehyde, stained with crystal violet, and counted under a microscope.

Flow cytometry and actin polymerization assays

For flow cytometry, 2×10^5 cells previously detached with 2 mM EDTA in PBS were incubated with different antibodies (10 μg/mL) in presence of human gamma globulin (20 μg/mL) in PBS for 30 min at 4ºC. After washing, cells were incubated with Alexa-Fluor 488 conjugated secondary antibodies (Thermo Fisher Scientific). Fluorescence was analyzed in a Coulter Epics XL cytofluorometer. At least 10,000 events per sample were acquired, and cells were identified on the basis of their specific forward and side light-scattering properties. For actin polymerization assays, cells were fixed with 7.4% formaldehyde, permeabilized with 1 mg/mL lysophosphatidylcholine, and stained with 1 μg/mL FITC-Phalloidin (Sigma-Aldrich). After washing, cells were analyzed as above.

Immunohistochemistry

Immunohistochemistry staining was carried out as previously described [46]. Anti-SOSTDC1 (Abcam) was used at 1:100 dilution and anti-ALCAM (R&D systems) at 1:50 dilution.

***In silico* analyses of SOSTDC1 sequence, structure and ALCAM expression**

438 See Supplementary Information

439 **Metastasis experiments in nude mice**

440 Mice experiments were approved by the ethics committee of Consejo Superior de
441 Investigaciones Científicas and the Community of Madrid (PROEX 252/15). Swiss nude
442 mice (Charles River; n = 6 per condition) were inoculated in the spleen with 5×10^5
443 KM12L4 cells in 25 μL PBS. Mice were inspected daily for signs of disease, such as
444 abdominal distension, locomotive deficit, or tumor detectable by palpation. When any such
445 sign was visible, mice were euthanized, analyzed by necropsy, and inspected for liver
446 metastasis.

447 **Statistical analysis**

448 Data with Gaussian distribution were analyzed by one-way ANOVA followed by Tukey-
449 Kramer multiple comparison test. Histograms showed the average of the assessed value,
450 whereas the error bars showed the standard deviation. Number of patients with metastasis
451 was assessed by chi-square test. Protein expressions in primary tumor and metastasis were
452 analyzed with Wilcoxon matched pairs test. Survival curves were plotted using a Kaplan–
453 Meier analysis and compared with the log-rank test. The minimum acceptable level of
454 significance in all tests was $P < 0.05$.

455 **Acknowledgements**

456 We thank Diego Laxalde, Alejandro Diaz, José Ramón Gutiérrez, Marcos Rodriguez, Eva
457 Calviño, and Gemma Elvira for their contributions to the manuscript. This research was
458 supported by grants from the Ministerio de Ciencia e Innovación (BIO2015-66489-R,

RTI2018-095055-B100), Foundation Ramón Areces and PRB3 (ISCIII-SGEFI/FEDER-PT17/0019/0008).

Author contributions

J.I.C. and R.A.B. designed the study, R.A.B., L.P., M.J., V.R., and J.I.I. carried out the experiments, R.A.B. and J.I.C. analyzed the data, J.I.I. provided reagents and protocols and R.A.B. and J.I.C. wrote the manuscript.

Conflict of interest

J.I.C. has stock ownership of Protein Alternatives SL. J.I.I. is employee of Protein Alternatives SL. All other authors have no conflict of interest to declare.

Supplementary information is available at Oncogene's website

REFERENCES

1 Lambert AW, Pattabiraman DR, Weinberg RA. Emerging Biological Principles of Metastasis. Cell 2017; 168: 670-691.

2 Reya T, Morrison SJ, Clarke MF, Weissman IL. Stem cells, cancer, and cancer stem cells. Nature 2001; 414: 105-111.

3 Oskarsson T, Batlle E, Massague J. Metastatic Stem Cells: Sources, Niches, and Vital Pathways. Cell Stem Cell 2014; 14: 306-321.

4 Morikawa K, Walker SM, Jessup JM, Fidler IJ. In vivo selection of highly metastatic cells from surgical specimens of different primary human colon carcinomas implanted into nude mice. Cancer Res 1988; 48: 1943-1948.

5 Bartolome RA, Barderas R, Torres S, Fernandez-Acenero MJ, Mendes M, Garcia-Foncillas J *et al*. Cadherin-17 interacts with alpha2beta1 integrin to regulate cell proliferation and adhesion in colorectal cancer cells causing liver metastasis. Oncogene 2014; 33: 1658-1669.

6 Kim GR, Ha GH, Bae JH, Oh SO, Kim SH, Kang CD. Metastatic colon cancer cell populations contain more cancer stem-like cells with a higher susceptibility to natural killer cell-mediated lysis compared with primary colon cancer cells. Oncol Lett 2015; 9: 1641-1646.

7 Barderas R, Mendes M, Torres S, Bartolome RA, Lopez-Lucendo M, Villar-Vazquez R *et al*. In-depth characterization of the secretome of colorectal cancer metastatic cells identifies key proteins in cell adhesion, migration, and invasion. Mol Cell Proteomics 2013; 12: 1602-1620.

8 Yanagita M, Oka M, Watabe T, Iguchi H, Niida A, Takahashi S *et al*. USAG-1: a bone morphogenetic protein antagonist abundantly expressed in the kidney. Biochem Biophys Res Commun 2004; 316: 490-500.

9 Nolan K, Thompson TB. The DAN family: modulators of TGF-beta signaling and beyond. Protein Sci 2014; 23: 999-1012.

10 Yanagita M. BMP antagonists: their roles in development and involvement in pathophysiology. Cytokine Growth Factor Rev 2005; 16: 309-317.

11 Lintern KB, Guidato S, Rowe A, Saldanha JW, Itasaki N. Characterization of wise protein and its molecular mechanism to interact with both Wnt and BMP signals. J Biol Chem 2009; 284: 23159-23168.

12 Blish KR, Wang W, Willingham MC, Du W, Birse CE, Krishnan SR *et al*. A human bone morphogenetic protein antagonist is down-regulated in renal cancer. Mol Biol Cell 2008; 19: 457-464.

13 Clausen KA, Blish KR, Birse CE, Triplette MA, Kute TE, Russell GB *et al*. SOSTDC1 differentially modulates Smad and beta-catenin activation and is down-regulated in breast cancer. Breast Cancer Res Treat 2011; 129: 737-746.

14 Tesfay L, Clausen KA, Kim JW, Hegde P, Wang X, Miller LD *et al*. Hepcidin regulation in prostate and its disruption in prostate cancer. Cancer Res 2015; 75: 2254-2263.

15 Liu L, Wu S, Yang Y, Cai J, Zhu X, Wu J *et al*. SOSTDC1 is down-regulated in non-small cell lung cancer and contributes to cancer cell proliferation. Cell Biosci 2016; 6: 24.

16 Chen G, Gong H, Wang T, Wang J, Han Z, Bai G *et al*. SOSTDC1 inhibits bone metastasis in non-small cell lung cancer and may serve as a clinical therapeutic target. Int J Mol Med 2018; 42: 3424-3436.

17 Cui Y, Zhang F, Jia Y, Sun L, Chen M, Wu S *et al*. The BMP antagonist, SOSTDC1, restrains gastric cancer progression via inactivation of c-Jun signaling. Am J Cancer Res 2019; 9: 2331-2348.

18 Gao H, Chakraborty G, Lee-Lim AP, Mo Q, Decker M, Vonica A *et al*. The BMP inhibitor Coco reactivates breast cancer cells at lung metastatic sites. Cell 2012; 150: 764-779.

19 Yan K, Wu Q, Yan DH, Lee CH, Rahim N, Tritschler I *et al*. Glioma cancer stem cells secrete Gremlin1 to promote their maintenance within the tumor hierarchy. Genes Dev 2014; 28: 1085-1100.

20 Calon A, Espinet E, Palomo-Ponce S, Tauriello DV, Iglesias M, Cespedes MV *et al*. Dependency of colorectal cancer on a TGF-beta-driven program in stromal cells for metastasis initiation. Cancer Cell 2012; 22: 571-584.

21 von Lersner A, Droesen L, Zijlstra A. Modulation of cell adhesion and migration through regulation of the immunoglobulin superfamily member ALCAM/CD166. Clin Exp Metastasis 2019; 36: 87-95.

22 Chappell PE, Garner LI, Yan J, Metcalfe C, Hatherley D, Johnson S *et al*. Structures of CD6 and Its Ligand CD166 Give Insight into Their Interaction. Structure 2015; 23: 1426-1436.

23 Yamaguchi H, Condeelis J. Regulation of the actin cytoskeleton in cancer cell migration and invasion. Biochim Biophys Acta 2007; 1773: 642-652.

24 Lunter PC, van Kilsdonk JW, van Beek H, Cornelissen IM, Bergers M, Willems PH *et al*. Activated leukocyte cell adhesion molecule (ALCAM/CD166/MEMD), a novel actor in invasive growth, controls matrix metalloproteinase activity. Cancer Res 2005; 65: 8801-8808.

25 van Kilsdonk JW, Wilting RH, Bergers M, van Muijen GN, Schalkwijk J, van Kempen LC *et al*. Attenuation of melanoma invasion by a secreted variant of activated leukocyte cell adhesion molecule. Cancer Res 2008; 68: 3671-3679.

26 Rawat A, Gopisetty G, Thangarajan R. E4BP4 is a repressor of epigenetically regulated SOSTDC1 expression in breast cancer cells. Cell Oncol (Dordr) 2014; 37: 409-419.

27 Gopal G, Raja UM, Shirley S, Rajalekshmi KR, Rajkumar T. SOSTDC1 down-regulation of expression involves CpG methylation and is a potential prognostic marker in gastric cancer. Cancer Genet 2013; 206: 174-182.

28 Zhou Q, Chen J, Feng J, Xu Y, Zheng W, Wang J. SOSTDC1 inhibits follicular thyroid cancer cell proliferation, migration, and EMT via suppressing PI3K/Akt and MAPK/Erk signaling pathways. Mol Cell Biochem 2017; 435: 87-95.

29 Secondini C, Wetterwald A, Schwaninger R, Thalmann GN, Cecchini MG. The role of the BMP signaling antagonist noggin in the development of prostate cancer osteolytic bone metastasis. PLoS One 2011; 6: e16078.

30 Young RA. Control of the embryonic stem cell state. Cell 2011; 144: 940-954.

31 Ben-Porath I, Thomson MW, Carey VJ, Ge R, Bell GW, Regev A *et al*. An embryonic stem cell-like gene expression signature in poorly differentiated aggressive human tumors. Nat Genet 2008; 40: 499-507.

32 Dalerba P, Dylla SJ, Park IK, Liu R, Wang X, Cho RW *et al*. Phenotypic characterization of human colorectal cancer stem cells. Proc Natl Acad Sci U S A 2007; 104: 10158-10163.

33 Horst D, Kriegl L, Engel J, Kirchner T, Jung A. Prognostic significance of the cancer stem cell markers CD133, CD44, and CD166 in colorectal cancer. Cancer Invest 2009; 27: 844-850.

34 Weichert W, Knosel T, Bellach J, Dietel M, Kristiansen G. ALCAM/CD166 is overexpressed in colorectal carcinoma and correlates with shortened patient survival. J Clin Pathol 2004; 57: 1160-1164.

35 Donizy P, Zietek M, Halon A, Leskiewicz M, Kozyra C, Matkowski R. Prognostic significance of ALCAM (CD166/MEMD) expression in cutaneous melanoma patients. Diagn Pathol 2015; 10: 86.

36 Kahlert C, Weber H, Mogler C, Bergmann F, Schirmacher P, Kenngott HG *et al*. Increased expression of ALCAM/CD166 in pancreatic cancer is an independent prognostic marker for poor survival and early tumour relapse. Br J Cancer 2009; 101: 457-464.

37 Inaguma S, Lasota J, Wang Z, Czapiewski P, Langfort R, Rys J *et al*. Expression of ALCAM (CD166) and PD-L1 (CD274) independently predicts shorter survival in malignant pleural mesothelioma. Hum Pathol 2018; 71: 1-7.

38 Tudor C, te Riet J, Eich C, Harkes R, Smisdom N, Bouhuijzen Wenger J *et al*. Syntenin-1 and ezrin proteins link activated leukocyte cell adhesion molecule to the actin cytoskeleton. J Biol Chem 2014; 289: 13445-13460.

39 Gilsanz A, Sanchez-Martin L, Gutierrez-Lopez MD, Ovalle S, Machado-Pineda Y, Reyes R *et al*. ALCAM/CD166 adhesive function is regulated by the tetraspanin CD9. Cell Mol Life Sci 2013; 70: 475-493.

40 Rauhala HE, Teppo S, Niemela S, Kallioniemi A. Silencing of the ARP2/3 complex disturbs pancreatic cancer cell migration. Anticancer Res 2013; 33: 45-52.

41 Kholmanskikh SS, Dobrin JS, Wynshaw-Boris A, Letourneau PC, Ross ME. Disregulated RhoGTPases and actin cytoskeleton contribute to the migration defect in Lis1-deficient neurons. J Neurosci 2003; 23: 8673-8681.

42 Lo FY, Chen HT, Cheng HC, Hsu HS, Wang YC. Overexpression of PAFAH1B1 is associated with tumor metastasis and poor survival in non-small cell lung cancer. Lung Cancer 2012; 77: 585-592.

43 Weidle UH, Eggle D, Klostermann S, Swart GW. ALCAM/CD166: cancer-related issues. Cancer Genomics Proteomics 2010; 7: 231-243.

44 Devis L, Moiola CP, Masia N, Martinez-Garcia E, Santacana M, Stirbat TV *et al*. Activated leukocyte cell adhesion molecule (ALCAM) is a marker of recurrence and promotes cell migration, invasion, and metastasis in early-stage endometrioid endometrial cancer. J Pathol 2017; 241: 475-487.

45 Piazza T, Cha E, Bongarzone I, Canevari S, Bolognesi A, Polito L *et al*. Internalization and recycling of ALCAM/CD166 detected by a fully human single-chain recombinant antibody. J Cell Sci 2005; 118: 1515-1525.

46 Torres S, Garcia-Palmero I, Herrera M, Bartolome RA, Pena C, Fernandez-Acenero MJ *et al*. LOXL2 Is Highly Expressed in Cancer-Associated Fibroblasts and Associates to Poor Colon Cancer Survival. Clin Cancer Res 2015; 21: 4892-4902.

Legends to the figures

Figure 1. SOSTDC1 is overexpressed in colorectal cancer metastasis. A, Western blot analysis of distinct colorectal cancer cell lines (as indicated) of SOSTDC1 in the lysate or media (secreted) (top) and quantification (bottom); anti–α-tubulin was used as loading control. B, Left, Western blot analysis of SOSTDC1 expression in normal colon (C), primary tumor (T), normal liver (L), or liver metastasis (M) from colorectal cancer patients; anti-RhoGDI was used as loading control. Right, band quantification with averages $\pm$ standard errors are shown. SOSTDC1 expression was significantly enhanced in liver metastasis as compared to normal liver or primary tumor ($*P < 0.05$). C, Left, quantification of immunohistochemical analysis of SOSTDC1 in colon cancer samples of paired colon and liver tissues from the same patients; right, representative images. SOSTDC1 was significantly increased in liver metastasis as compared to primary tumor ($*P < 0.05$).

Figure 2. SOSTDC1 promotes cell invasion and activation of signaling pathways. A, Western blot verification of knockdown of SOSTDC1 in SW620, KM12SM, or KM12L4 cells, after cells were transfected with siRNAs or shRNA against SOSTDC1 or a control, as indicated; anti-RhoGDI was used as a loading control. B, C, Invasion assays in Matrigel of the indicated transfected cells (B) or in the presence of control or anti-SOSTDC1 antibodies (C). D, Western blot analysis of signaling pathways in SOSTDC1-silenced cells using the indicated antibodies; anti-RhoGDI was used as a loading control. **E,** Invasion assays of the indicated cells towards SOSTDC1 (10 ng/ml) in the presence of different inhibitors (bottom). Cell invasion was significantly inhibited by SOSTDC1 silencing or anti-SOSTDC1 antibodies ($*P < 0.05$; $**P < 0.01$; $***P < 0.001$).

Figure 3. SOSTDC1 inhibits BMP4 to maintain expression of stem cell transcription factors. A, A, Invasion assays of the SOSTDC1-silenced or control KM12L4 cells towards SOSTDC1 (10 ng/ml) in the presence of different BMP4 concentrations. SOSTDC1-mediated induction of invasive cells was reduced by BMP4 $**P < 0.01$; $***P < 0.001$. B, Semi-quantitative RT-PCR analysis of the indicated BMP receptors in the metastatic colorectal cancer cell lines (top left); GAPDH was amplified as loading control. Western blot analysis of the cell lines silenced or not for SOSTDC1 and treated with different

concentrations of BMP4; phospho-SMAD5 and total SMAD5 were detected. **C**, Colony formation assays of KM12SM cells in the presence of SOSTDC1 +/– BMP4 at the indicated concentrations. **D**, Relative expression of indicated genes after Q-PCR from SOSTDC1-silenced or control KM12L4 cells +/– BMP4. SOSTDC1-silenced cells treated with BMP4 (10 ng/mL) showed a significant reduction of the indicated genes or increase in the mRNA expression levels. $^{**}P < 0.01$; $^{***}P < 0.001$.

Figure 4. SOSTDC1 interacts with ALCAM using a CD6-like motif. A, **B,** SW620 cell lysates were immunoprecipitated using anti-SOSTDC1 or control antibodies. After SOSTDC1 immunoprecipitation, trypsin-digested immunoprecipitate peptides were analyzed by nanoLC-MS/MS (**A**) and identified protein were verified by Western blot (**B**). **C**, Sequence comparison of ALCAM-binding motifs in CD6 and SOSTDC1. **D**, *In silico* model of SOSTDC1 showing the location of ALCAM-binding sequences. **E**, Confocal microscopy of SW620 cells showing co-localization of ALCAM and SOSTDC1 in the cell membrane. **F**, Western blot verifying the knockdown of ALCAM expression in lysates from SW620 or KM12SM cells transfected with ALCAM or control siRNAs. **G**, Flow cytometry assays to detect the surface expression of SOSTDC1 and ALCAM in cell transfectants; the mean fluorescence intensity for each marker is shown.

Figure 5. Truncation of SOSTDC1 N-terminus inhibits ALCAM-mediated migration and invasion. A–C, SW620 or KM12SM cells were treated with SOSTDC1 or ΔN67-SOSTDC1 (10 ng/ml) and analyzed by flow cytometry to detect SOSTDC1 binding (**A**), invasion assays through Matrigel towards SOSTDC1 or ΔN67-SOSTDC1 (**B**), and actin polymerization assays (**C**). SOSTDC1 significantly increased, and ΔN67-SOSTDC1 significantly decreased, SOSTDC1 detection in cell surface, cell invasion, and F-actin content. $^{*}P < 0.05$; $^{**}P < 0.01$; $^{***}P < 0.001$. **D,** Western blot analysis of the indicated cells lines exposed to SOSTDC or ΔN67-SOSTDC1 for the indicated times; the antibodies used to detect signaling pathways are indicated.

Figure 6. ALCAM regulates cell invasion and actin polymerization in a coordinated way with SOSTDC1. A, Western blot of lysates from the indicated cell lines transfected with ALCAM or control siRNA, to verify ALCAM silencing. **B, C**, Cell invasion assays of SW620 or KM12SM cells transfected with SOSTDC1 and/or ALCAM siRNAs were

analyzed by cell invasion assays (B) and flow cytometry after F-actin polymerization assays (showing mean intensity fluorescence) (C) *$P < 0.05$. **C, D**, Western blots using the indicated antibodies of lysates from SW620 and KM12SM cells transfected with ALCAM or control siRNA and not treated (C) or treated with SOSTDC1 (10 ng/ml) (D). **E**, Western blot of anti-ALCAM or control antibody immunoprecipitates from SW620 cell lysates, using the indicated antibodies. **F**, Immunohistochemistry of ALCAM in colon cancer samples of paired primary tumors and liver metastasis from the same patients. Representative images of ALCAM staining intensity are shown. ALCAM expression significantly increased in liver metastasis compared to primary tumors. *$P < 0.05$.

Figure 7. SOSTDC1/ALCAM expression correlates with liver metastasis. A functional model. A, Percentage of patients with liver metastasis according to their expression levels of SOSTDC1 or ALCAM. High expression of SOSTDC1 or ALCAM increased significantly the percentage of patients with metastasis. *$P < 0.05$. **B**, Kaplan–Meier survival of mice inoculated in the spleen with KM12L4 cells stably transfected with control or SOSTDC1 shRNA. Survival time was significantly enhanced in mice inoculated with SOSTDC1 silenced cells. *$P < 0.05$. **C,** Quantification of liver metastasis volume from the inoculated mice of (B); averages $\pm$ standard deviation are shown. Liver colonization decreased significantly in mice inoculated with SOSTDC1 silenced cells. ***$P < 0.001$. **D,** A functional model of mechanisms involving SOSTDC1 during tumor progression.

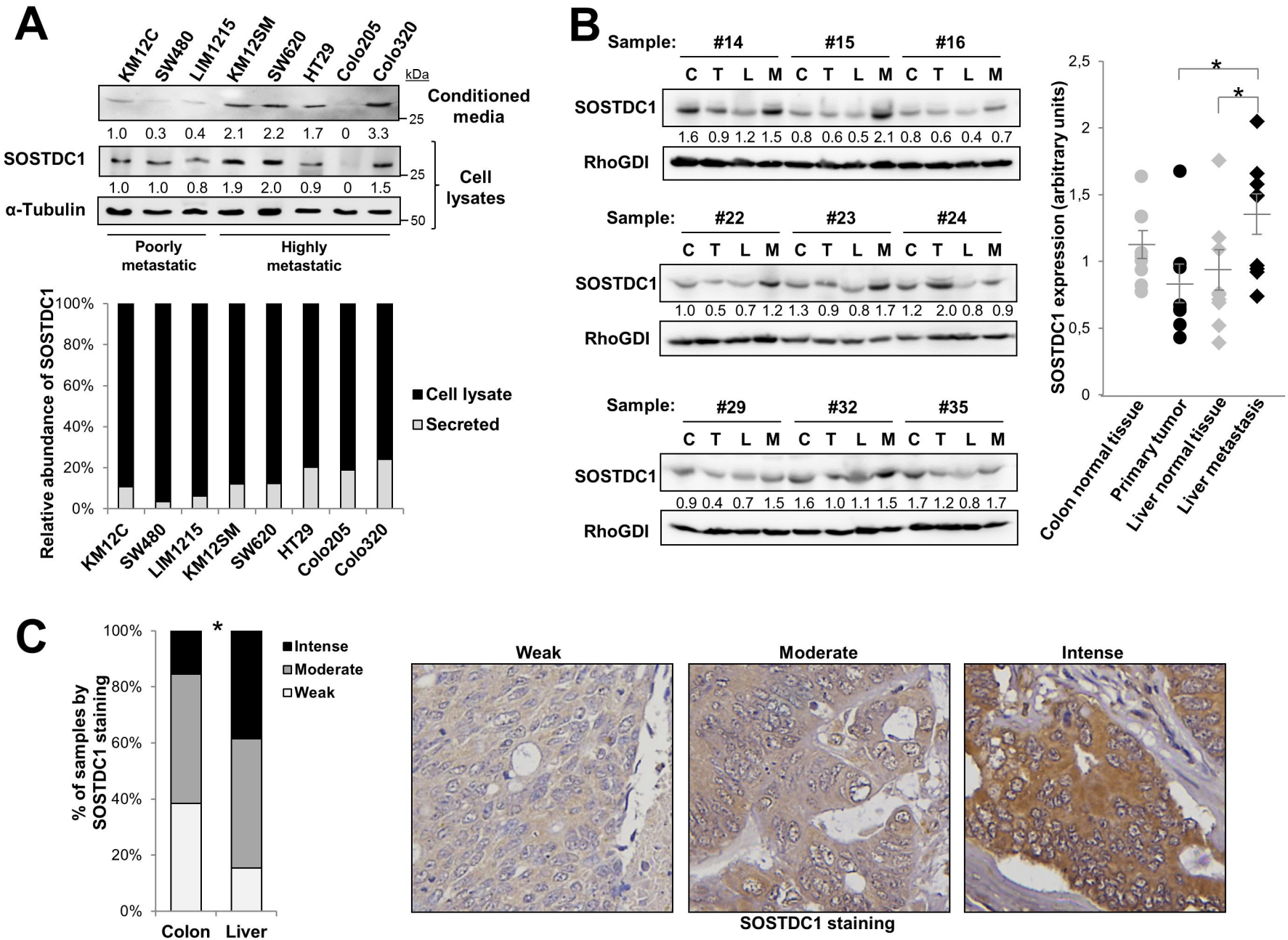
A
KM12C SW480 LIM1215 KM12SM SW620 HT29 Colo205 Colo320
kDa
Conditioned media
25
1.0 0.3 0.4 2.1 2.2 1.7 0 3.3
SOSTDC1
25
Cell lysates
1.0 1.0 0.8 1.9 2.0 0.9 0 1.5
α-Tubulin
50
Poorly metastatic
Highly metastatic
Relative abundance of SOSTDC1
100%
80%
60%
40%
20%
0%
Cell lysate
Secreted
KM12C SW480 LIM1215 KM12SM SW620 HT29 Colo205 Colo320
B
Sample: #14 #15 #16
C T L M C T L M C T L M
SOSTDC1
1.6 0.9 1.2 1.5 0.8 0.6 0.5 2.1 0.8 0.6 0.4 0.7
RhoGDI
Sample: #22 #23 #24
C T L M C T L M C T L M
SOSTDC1
1.0 0.5 0.7 1.2 1.3 0.9 0.8 1.7 1.2 2.0 0.8 0.9
RhoGDI
Sample: #29 #32 #35
C T L M C T L M C T L M
SOSTDC1
0.9 0.4 0.7 1.5 1.6 1.0 1.1 1.5 1.7 1.2 0.8 1.7
RhoGDI
SOSTDC1 expression (arbitrary units)
2,5
2
1,5
1
0,5
0
*
*
Colon normal tissue
Primary tumor
Liver normal tissue
Liver metastasis
C
100%
80%
60%
40%
20%
0%
% of samples by SOSTDC1 staining
*
Intense
Moderate
Weak
Colon
Liver
Weak
Moderate
Intense
SOSTDC1 staining

Fig. 1

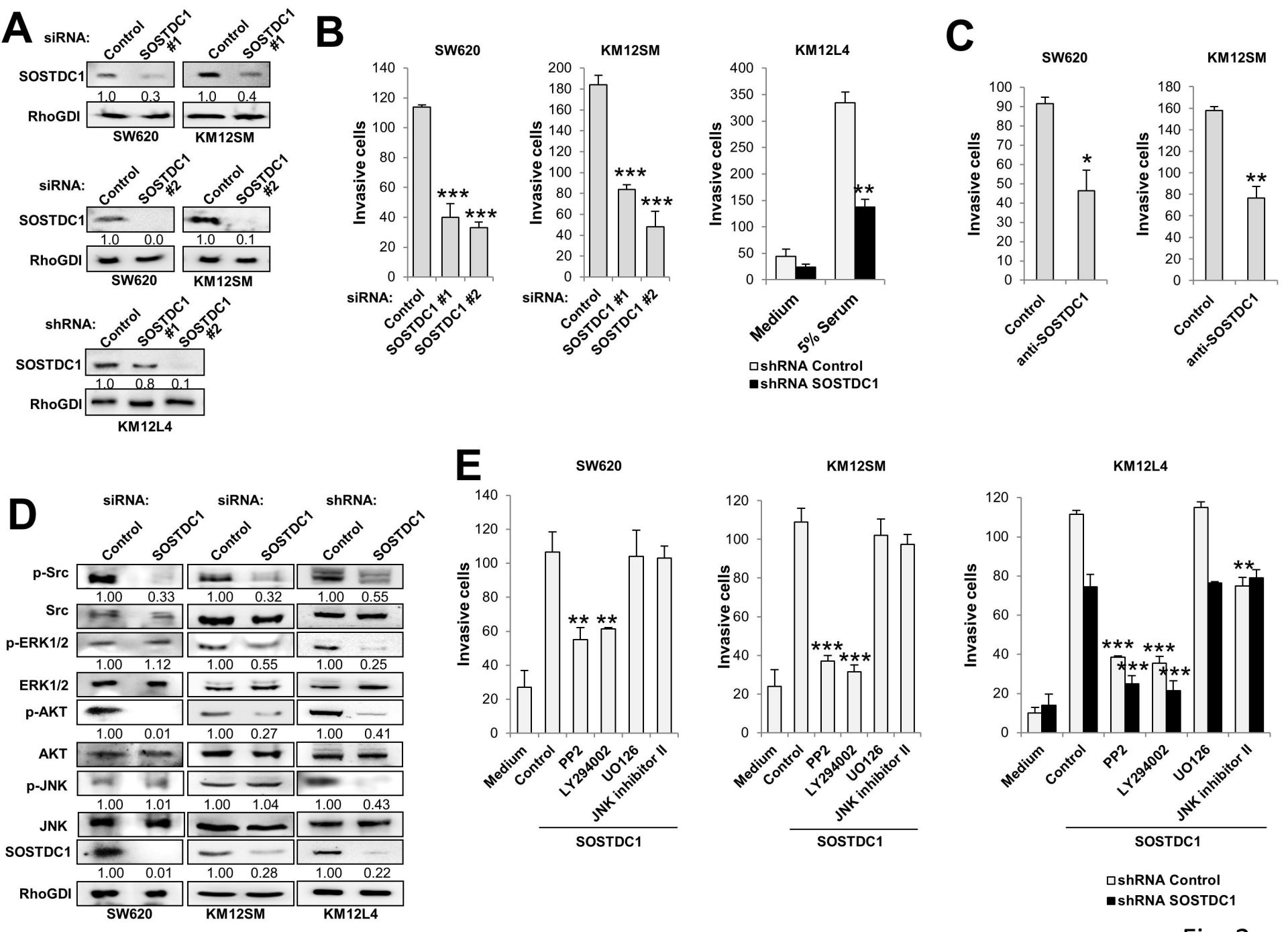
A
siRNA:
Control
SOSTDC1 #1
SOSTDC1
SOSTDC1
1.0 0.3
1.0 0.4
RhoGDI
SW620
KM12SM
siRNA:
SOSTDC1 #2
1.0 0.0
1.0 0.1
shRNA:
SOSTDC1 #1
SOSTDC1 #2
1.0 0.8 0.1
KM12L4
B
SW620
KM12SM
KM12L4
Invasive cells
siRNA:
Control
SOSTDC1 #1
SOSTDC1 #2
Medium
5% Serum
shRNA Control
shRNA SOSTDC1
C
SW620
KM12SM
Invasive cells
Control
anti-SOSTDC1
D
siRNA:
siRNA:
shRNA:
Control
SOSTDC1
p-Src
1.00 0.33
1.00 0.32
1.00 0.55
Src
p-ERK1/2
1.00 1.12
1.00 0.55
1.00 0.25
ERK1/2
p-AKT
1.00 0.01
1.00 0.27
1.00 0.41
AKT
p-JNK
1.00 1.01
1.00 1.04
1.00 0.43
JNK
SOSTDC1
1.00 0.01
1.00 0.28
1.00 0.22
RhoGDI
SW620
KM12SM
KM12L4
E
SW620
KM12SM
KM12L4
Invasive cells
Medium
Control
PP2
LY294002
UO126
JNK inhibitor II
SOSTDC1
shRNA Control
shRNA SOSTDC1

Fig. 2

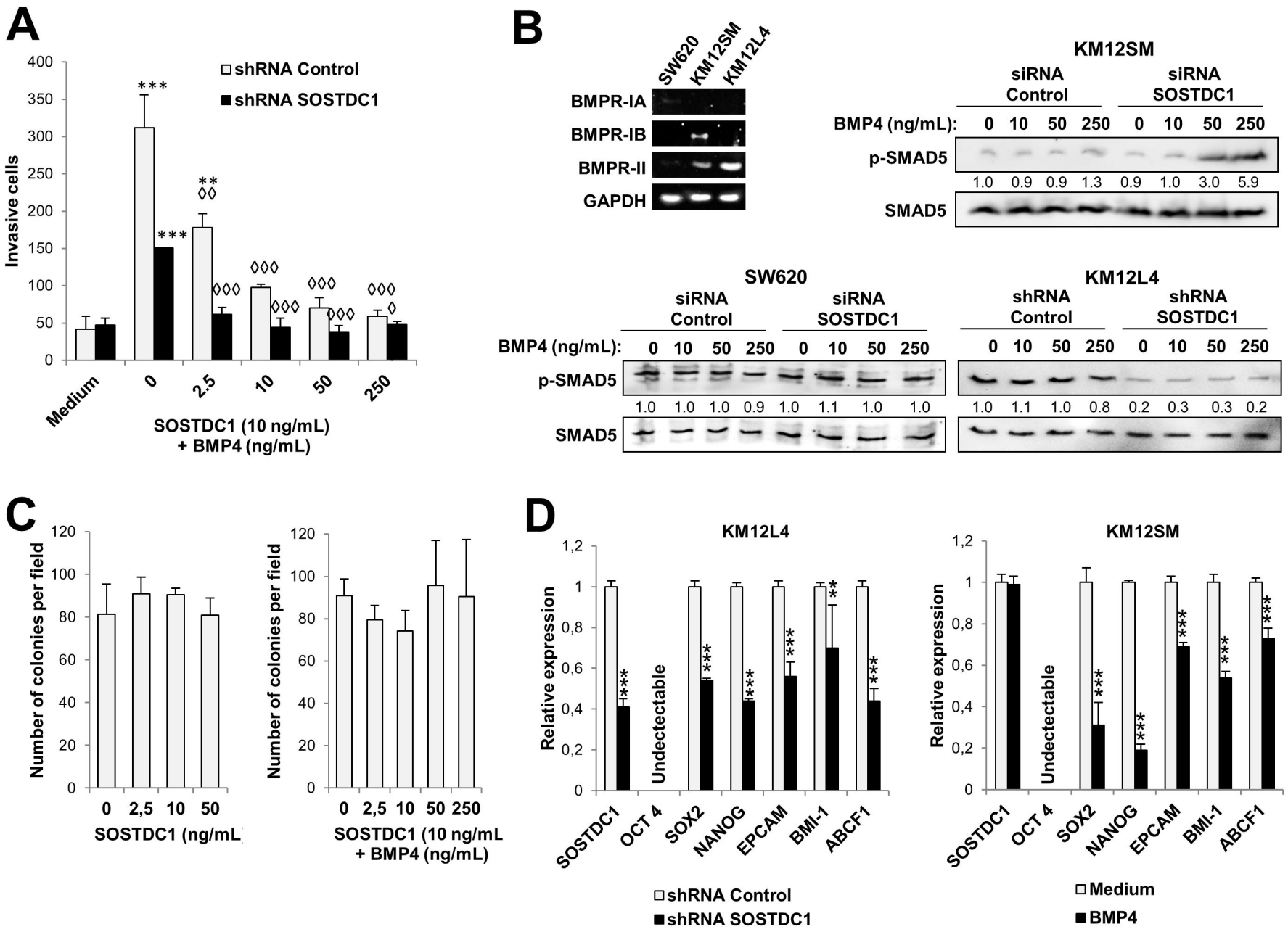
A
shRNA Control
shRNA SOSTDC1
Invasive cells
400
350
300
250
200
150
100
50
0
***
***
**
◊◊
◊◊◊
◊◊◊
◊◊◊
◊◊◊
◊
Medium
0
2.5
10
50
250
SOSTDC1 (10 ng/mL)
+ BMP4 (ng/mL)
B
SW620
KM12SM
KM12L4
BMPR-IA
BMPR-IB
BMPR-II
GAPDH
KM12SM
siRNA Control
siRNA SOSTDC1
BMP4 (ng/mL): 0 10 50 250 0 10 50 250
p-SMAD5
1.0 0.9 0.9 1.3 0.9 1.0 3.0 5.9
SMAD5
SW620
siRNA Control
siRNA SOSTDC1
BMP4 (ng/mL): 0 10 50 250 0 10 50 250
p-SMAD5
1.0 1.0 1.0 0.9 1.0 1.1 1.0 1.0
SMAD5
KM12L4
shRNA Control
shRNA SOSTDC1
0 10 50 250 0 10 50 250
1.0 1.1 1.0 0.8 0.2 0.3 0.3 0.2
C
Number of colonies per field
120
100
80
60
40
20
0
0 2,5 10 50
SOSTDC1 (ng/mL)
Number of colonies per field
0 2,5 10 50 250
SOSTDC1 (10 ng/mL
+ BMP4 (ng/mL)
D
KM12L4
Relative expression
1,2
1
0,8
0,6
0,4
0,2
0
***
Undectectable
***
***
***
**
***
SOSTDC1
OCT 4
SOX2
NANOG
EPCAM
BMI-1
ABCF1
shRNA Control
shRNA SOSTDC1
KM12SM
Relative expression
Undectectable
***
***
***
***
***
SOSTDC1
OCT 4
SOX2
NANOG
EPCAM
BMI-1
ABCF1
Medium
BMP4

Fig. 3

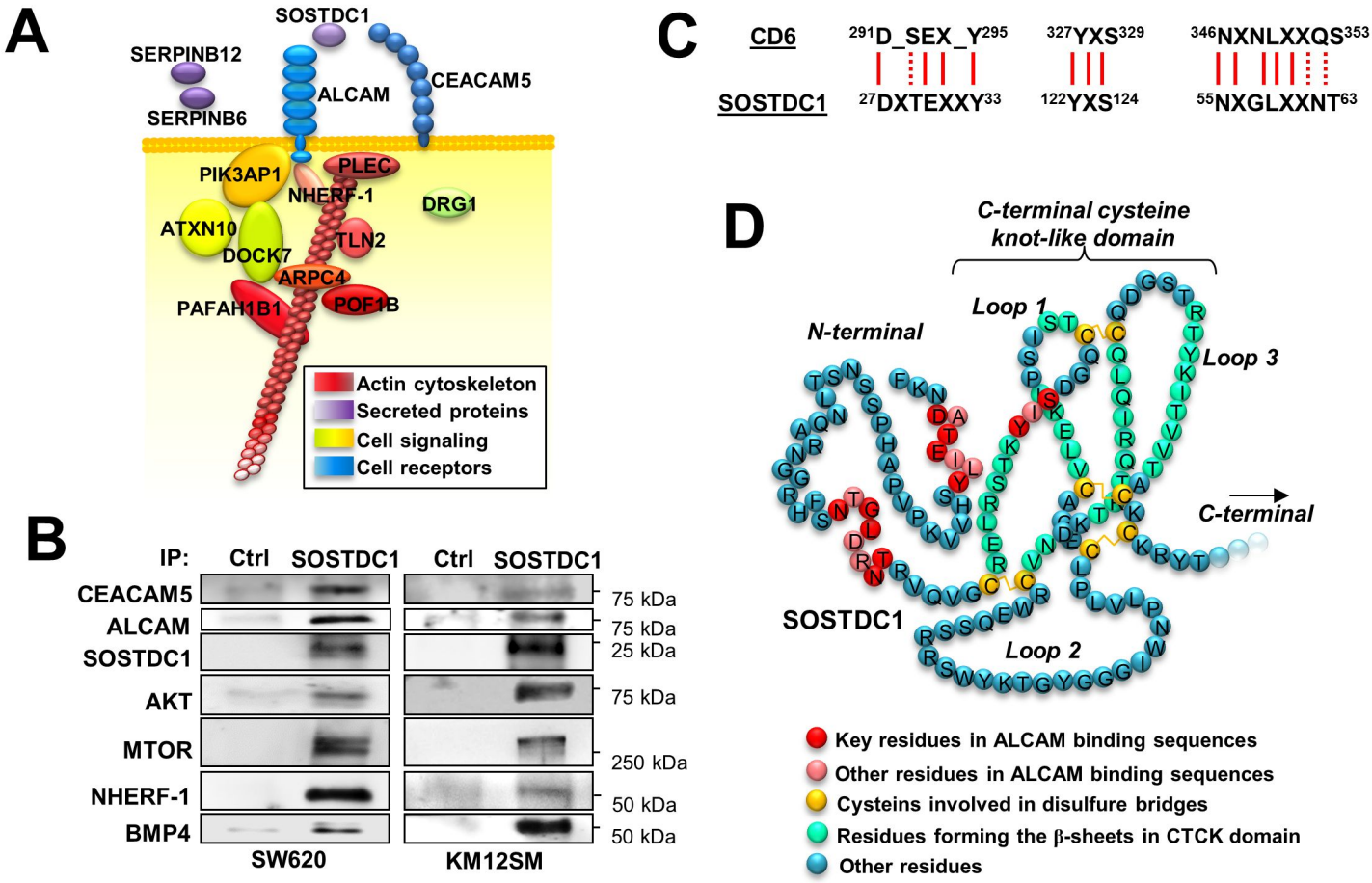
A
SOSTDC1
SERPINB12
SERPINB6
ALCAM
CEACAM5
PIK3AP1
PLEC
NHERF-1
DRG1
ATXN10
TLN2
DOCK7
ARPC4
PAFAH1B1
POF1B
Actin cytoskeleton
Secreted proteins
Cell signaling
Cell receptors
C
CD6
291D_SEX_Y295
327YXS329
346NXNLXXQS353
SOSTDC1
27DXTEXXY33
122YXS124
55NXGLXXNT63
B
IP: Ctrl SOSTDC1 Ctrl SOSTDC1
CEACAM5
ALCAM
SOSTDC1
AKT
MTOR
NHERF-1
BMP4
75 kDa
75 kDa
25 kDa
75 kDa
250 kDa
50 kDa
50 kDa
SW620
KM12SM
D
C-terminal cysteine knot-like domain
N-terminal
Loop 1
Loop 3
C-terminal
SOSTDC1
Loop 2
Key residues in ALCAM binding sequences
Other residues in ALCAM binding sequences
Cysteins involved in disulfure bridges
Residues forming the β-sheets in CTCK domain
Other residues
E
DAPI
ALCAM
SOTDC1
Co-localization
25 μm
Co-localization: 77.1% ± 1.8%
Pearson's Correlation: 0.81
Overlap Coefficient: 0.81
F
siRNA: Ctrl ALCAM
ALCAM
1.0 0.5
RhoGDI
SW620
siRNA: Ctrl ALCAM
ALCAM
1.0 0.4
RhoGDI
KM12SM
G
SW620
siRNA Control
siRNA ALCAM
2.88
1.59
21.8
11.4
KM12SM
siRNA Control
siRNA ALCAM
SOSTDC1 expression
3.36
0.98
ALCAM expression
46.8
17.9
Cell number
0 10 100 10000 10 100 1000
0 10 100 1000 0 10 100 1000
Fluorescence intensity
Fluorescence intensity

Fig. 4

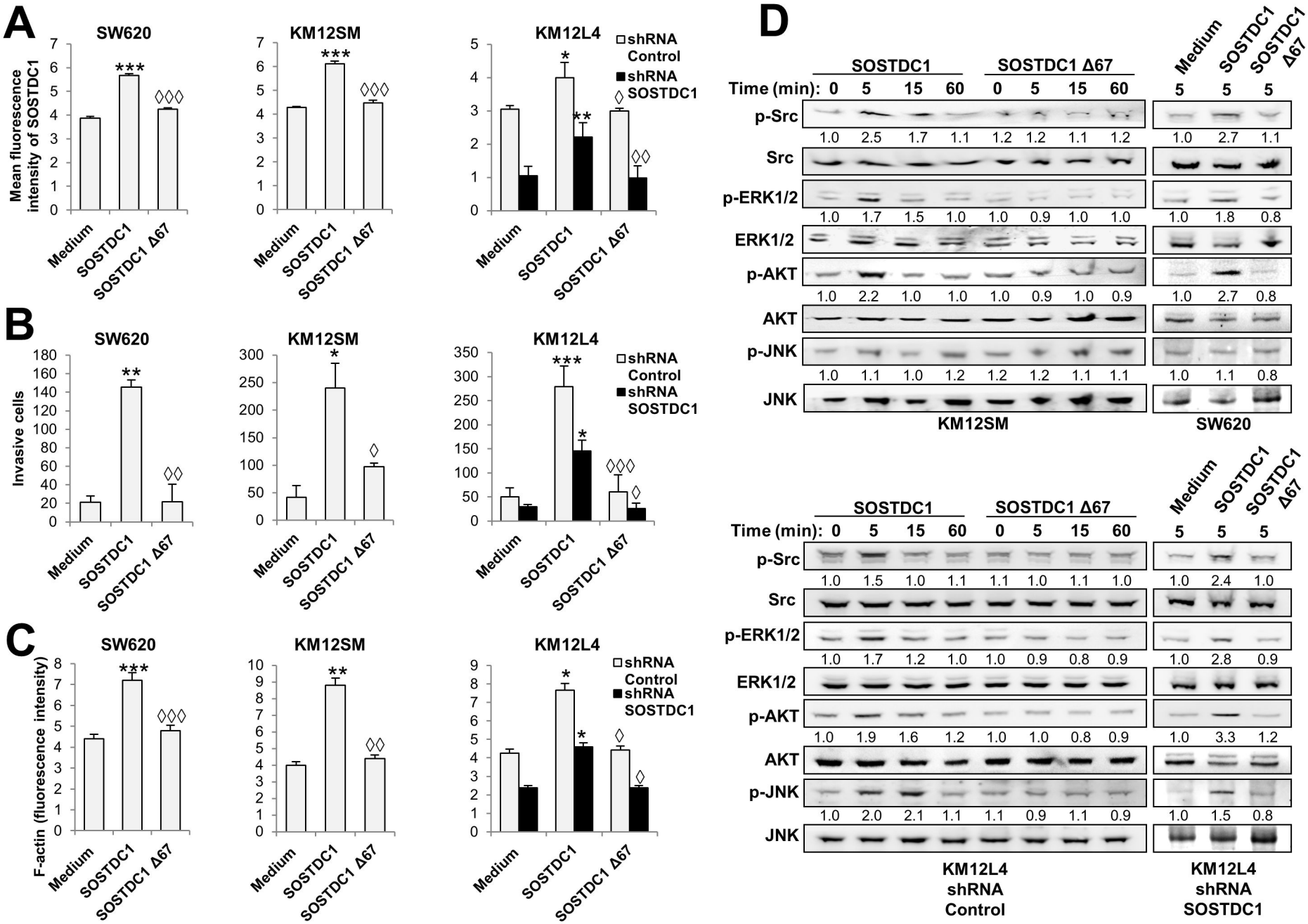
A
SW620
KM12SM
KM12L4
Mean fluorescence intensity of SOSTDC1
shRNA Control
shRNA SOSTDC1
Medium
SOSTDC1
SOSTDC1 Δ67
B
Invasive cells
C
F-actin (fluorescence intensity)
D
SOSTDC1
SOSTDC1 Δ67
Time (min): 0 5 15 60 0 5 15 60
Medium
SOSTDC1
SOSTDC1 Δ67
5 5 5
p-Src
Src
p-ERK1/2
ERK1/2
p-AKT
AKT
p-JNK
JNK
KM12SM
SW620
KM12L4 shRNA Control
KM12L4 shRNA SOSTDC1

Fig. 5

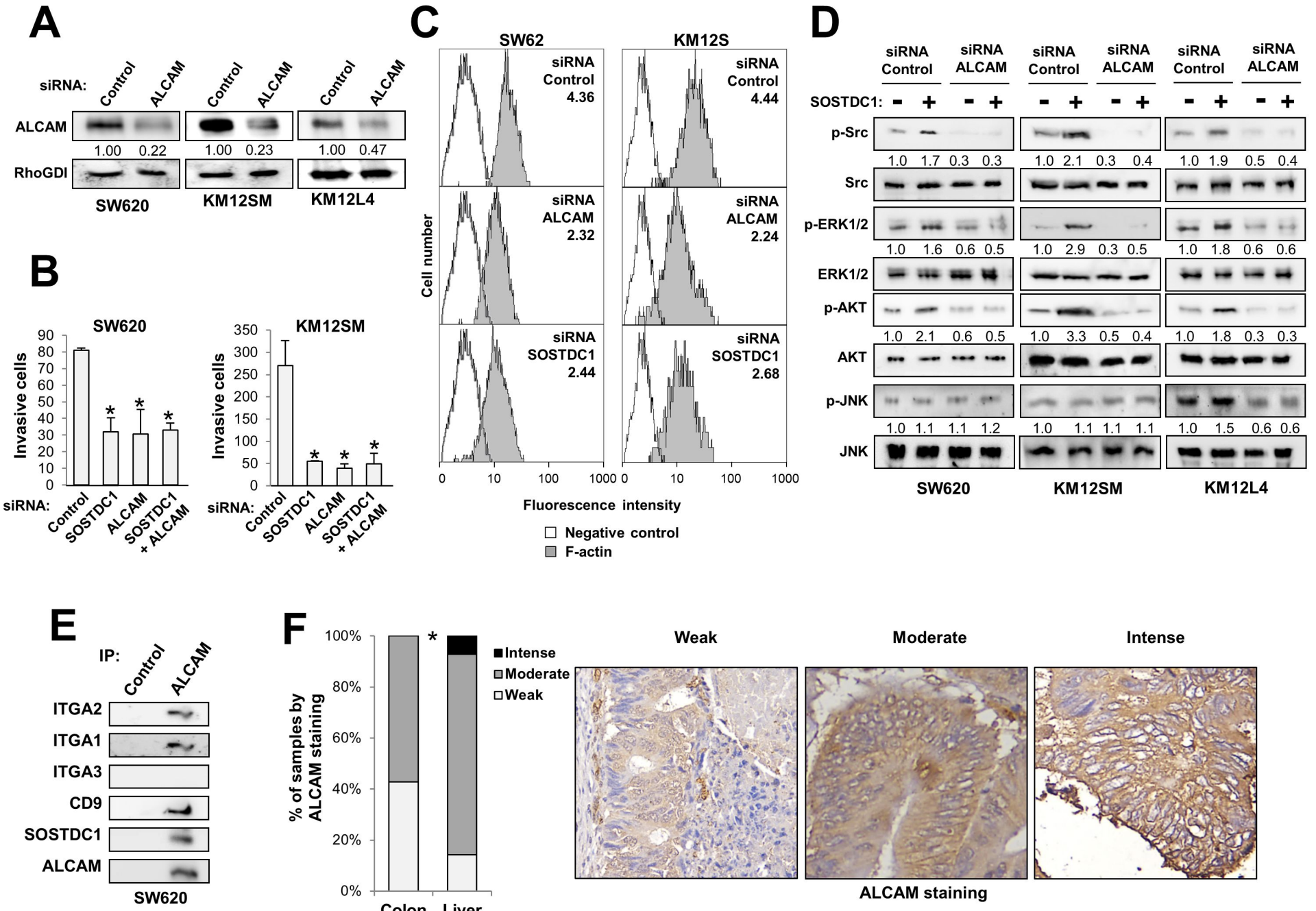
A
siRNA:
Control
ALCAM
ALCAM
1.00 0.22
1.00 0.23
1.00 0.47
RhoGDI
SW620
KM12SM
KM12L4
B
SW620
KM12SM
Invasive cells
siRNA:
Control
SOSTDC1
ALCAM
SOSTDC1 + ALCAM
C
SW62
KM12S
siRNA Control 4.36
siRNA Control 4.44
siRNA ALCAM 2.32
siRNA ALCAM 2.24
siRNA SOSTDC1 2.44
siRNA SOSTDC1 2.68
Cell number
Fluorescence intensity
Negative control
F-actin
D
siRNA Control
siRNA ALCAM
SOSTDC1:
p-Src
Src
p-ERK1/2
ERK1/2
p-AKT
AKT
p-JNK
JNK
SW620
KM12SM
KM12L4
E
IP:
Control
ALCAM
ITGA2
ITGA1
ITGA3
CD9
SOSTDC1
ALCAM
SW620
F
% of samples by ALCAM staining
Intense
Moderate
Weak
Colon
Liver
Weak
Moderate
Intense
ALCAM staining

Fig. 6

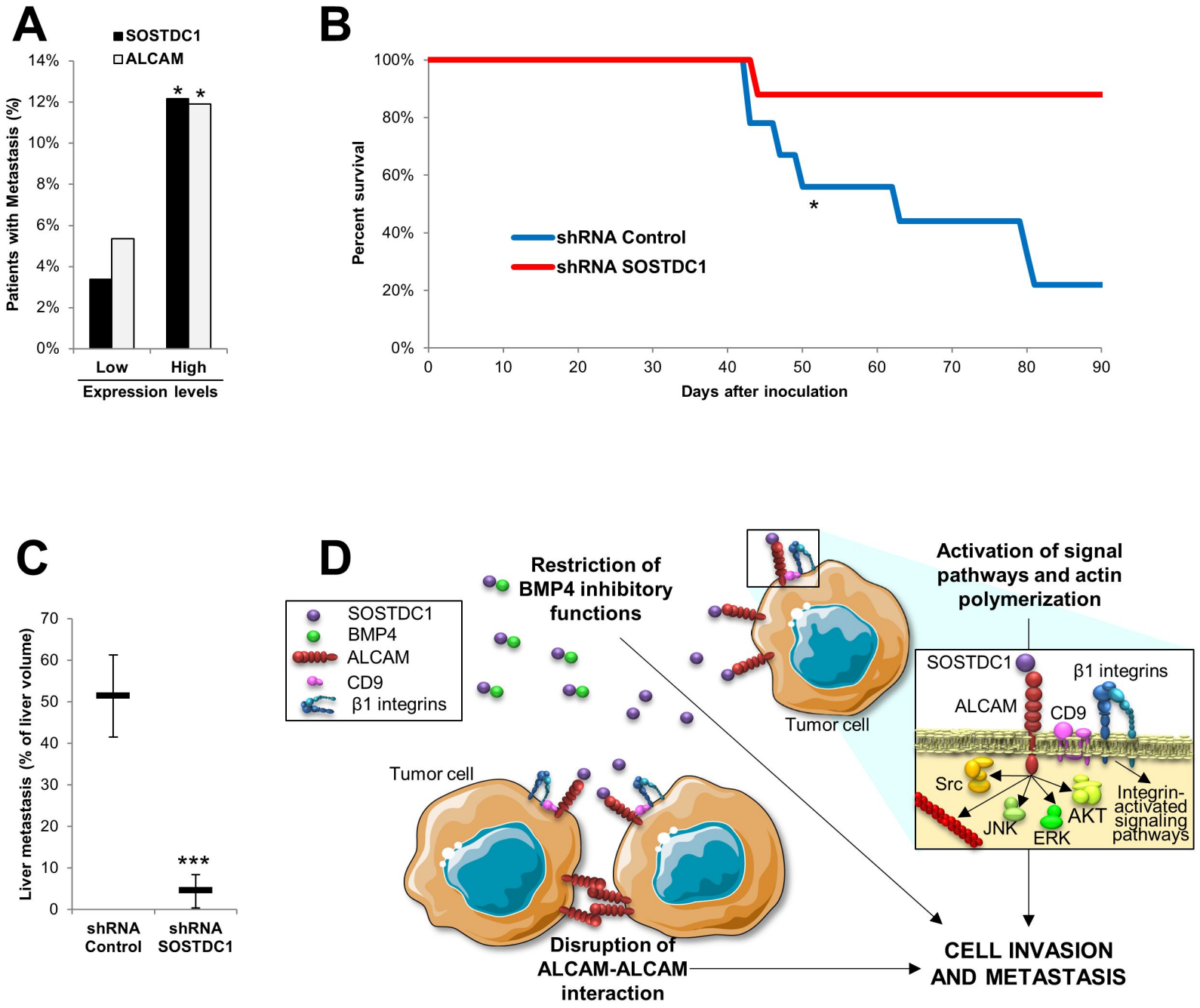
A
SOSTDC1
ALCAM
Patients with Metastasis (%)
14%
12%
10%
8%
6%
4%
2%
0%
*
*
Low
High
Expression levels
B
Percent survival
100%
80%
60%
40%
20%
0%
shRNA Control
shRNA SOSTDC1
*
0
10
20
30
40
50
60
70
80
90
Days after inoculation
C
Liver metastasis (% of liver volume)
70
60
50
40
30
20
10
0
***
shRNA Control
shRNA SOSTDC1
D
SOSTDC1
BMP4
ALCAM
CD9
β1 integrins
Restriction of BMP4 inhibitory functions
Tumor cell
Activation of signal pathways and actin polymerization
SOSTDC1
β1 integrins
ALCAM
CD9
Src
JNK
ERK
AKT
Integrin-activated signaling pathways
Tumor cell
Disruption of ALCAM-ALCAM interaction
CELL INVASION AND METASTASIS

Fig. 7